Electronic Supplementary Material (ESI) for ChemComm.

A sensitive turn-on fluorescence probe for intracellular imaging of glutathione using single-layer MnO_2 nanosheets-quenched fluorescent carbon quantum dots

Dinggeng He, Xiaoxiao Yang, Xiaoxiao He,* Kemin Wang,* Xue Yang, Xing He and Zhen Zou

State Key Laboratory of Chemo/Biosensing and Chemometrics, College of Chemistry and Chemical Engineering, College of Biology, Hunan University, Key Laboratory for Bio-Nanotechnology and Molecular Engineering of Hunan Province, Changsha 410082, China.

*E-mail: kmwang@hnu.edu.cn; xiaoxiaohe@hnu.edu.cn.

EXPERIMENTAL SECTION

Materials. Manganese chloride tetrahydrate ($MnCl_2$•$4H_2O$), hydrogen peroxide (H_2O_2, 30 wt%), tetramethylammonium hydroxide pentahydrate (TMA•OH), L-cysteine (Cys) and L-glutathione reduced (GSH) were purchased from Alfa Aesar (China). 3-[4,5-dimethylthialzol-2-yl]-2,5-diphenyltetrazolium bromid (MTT) and DL-homocysteine (HCys) were purchased from Sigma-Aldrich (USA). Dimethyl sulfoxide (DMSO) was obtained from Xilong reagent company (Guangdong, China). Citric acid monohydrate was obtained from Shanghai Shiyi Chemicals Reagent Co., Ltd. (China) and urea was obtained from Sinopharm Chemicals Reagent Co., Ltd. (China). All chemicals were of analytical grade and were used as received without further purification. All aqueous solutions were prepared using ultrapure water, which was prepared through a Millipore Milli-Q water purification system, with an electrical resistance >18.2 MΩ.

Apparatus and characterization. Ultraviolet-visible light (UV-vis) absorption spectra were recorded on a UV-2600 UV-vis spectrometer (Shimadzu, Japan) in the range of 200-700 nm. Fluorescence spectra were collected using a Hitachi Model F-7000 Fluorometer (Hitachi Co., Ltd., Japan). The samples were excited at 350 nm and the fluorescence emission ranged from 365 nm to 600 nm, in steps of 1 nm and fluorescence measurements were performed at room temperature under ambient conditions. Atomic force microscopy (AFM) images of samples were analyzed on a Multimode 8 (Bruker, USA). Transmission electron microscope image was obtained on a F20 field-emission transmission electron microscope and an accelerating voltage of 200 KV. Zeta potential and DLS measurements were performed at 25°C using a Nano ZS90 laser particle analyzer (Malvern Instruments, UK), equipped with a He-Ne laser (633 nm) at a fixed scattering angle of 90°. Fourier transform infrared (FT-IR) spectra were obtained from a TENSOR 27 spectrometer (Bruker Instruments Inc., Germany) in the range of 4000-400 cm^{-1}. The MTT assay was obtained in a Benchmark Plus, Biorad Instruments Inc, Japan. The confocal laser scanning

microscopy (CLSM) images were obtained on a Fluoview FV500, Olympus.

Synthesis of MnO_2 nanosheets. Single-layer MnO_2 nanosheets were synthesized according to a literature procedure reported previously.[1] In a typical reaction, 20 mL of mixture containing 0.6 M TMA•OH and 3.0 wt% H_2O_2 were added to 10 mL aqueous solution of 0.3 M $MnCl_2$•$4H_2O$ within 15 s. The resulting mixture a dark brown suspension was formed, then the product was stirred vigorously overnight in the open air at room temperature, which was accompanied by the generation of oxygen. Subsequently, the crude product was collected by centrifugation at 10000 rpm for 10 min, washed with alcohol and water several times and finally the solid was then placed under high vacuum at -60 °C for 12 h to remove the residual solvent. To acquire 1 mg mL^{-1} MnO_2 solution, 30 mg MnO_2 solid was dispersed in 30 mL ultrapure water and was degraded by ultrasonic cleaning machine and ultrasonic cell crasher.

Preparation of nitrogen-doped fluorescent carbon quantum dots (CQDs). Here, the CQDs were compounded utilizing microwave synthesis methods.[2] 10 mL mixture containing 3 g citric acid monohydrate and 3 g urea were then heated for about 4 min in a domestic 800 W microwave oven, after the solution changed from a colorless liquid to a dark-brown clustered solid, suggesting that the crude product was formed. Afterwards, the solid was then heated at 60 °C vacuum oven for 1 h to remove the remaining small molecules. Then the solid was redispersed in 20 mL of ultrapure water. After that the aqueous solution of the CQDs was purified by centrifugation at 3000 rpm for 20 min to remove large or agglomerated particles. The concentration of CQDs solution was acquired by dried 1 mL CQDs solution in 80 °C revolve vacuum oven for 4 h and the solution was diluted according to the demand.

Fluorescence quenching of the single-layer MnO_2 nanosheets toward CQDs. On the basis of the procedure above, various concentrations MnO_2 nanosheets (0 to 100 μg mL^{-1}) were added into CQDs (2.4 μg mL^{-1}) reaching a total volume of 200 μL

for each sample. The fluorescence detections were performed.

Analysis of GSH in aqueous solutions. For fluorescent sensing detection of GSH solution, the turn-on fluorescence probe based on MnO_2-CQDs nanocomposite was first prepared by hybridized MnO_2 nanosheets (30 μg mL^{-1}) with CQDs (2.4 μg mL^{-1}), and then various concentrations of GSH (0 to 200 μM) were added into MnO_2-CQDs nanocomposite, respectively, reaching a total volume of 200 μL for each sample. The mixtures were incubated at room temperature for 5 min and then the fluorescence detections were performed.

Selectivity of the fluorescence nanocomposite probe toward GSH. To explore the selectivity of the fluorescence probe toward GSH. Different electrolytes or biomolecules (KCl, NaCl, Na_2SO_4, $MgSO_4$, $MnCl_2$, Gly, Glu, Glucose, Sucrose, BSA, Cys, HCys and GSH) were added into MnO_2-CQDs nanocomposite solutions, respectively, reaching a total volume of 200 μL for each sample. After being incubation with GSH (200 and 500 μM), and different electrolytes and biomolecules (1 mM for each; 1 mg mL^{-1} for BSA, 500 μM for Cys, HCys) for 5 min at room temperature, fluorescence intensities of MnO_2-CQDs nanocomposite solutions were detected.

Cytotoxicity experiment. The cytotoxicity of MnO_2-CQDs nanocomposite and CQDs were evaluated by an MTT assay using HeLa cells. HeLa cells were cultured in 96-well plates at a density of 7×10^3 cells per well in 200 μL of medium containing 10% fetal bovine serum (FBS) and incubated at 37 °C and 5% CO_2. After grown for 24 h, various concentrations of MnO_2-CQDs nanocomposite (0-100 μg mL^{-1}) and CQDs (0-120 μg mL^{-1}) in culture medium were added into each well and then incubated for 24 h. MTT was used to assess cell viability. The MTT solution (0.5 mg mL^{-1}) was further incubated with cells in fresh medium for another 4 h. Then the medium was withdrawn and 150 μL of DMSO was added into each well to dissolve the precipitated formazan violet crystals at 37 °C for 10 min. The absorbance was

measured at 490 nm by a multidetection microplate reader.

Cell imaging. HeLa cells were maintained at 37 °C in 5% CO_2 in RPMI media. The cells were plated at around 60-70% confluency 24 h before imaging experiments in 35-mm culture dishes. Prior to imaging experiments, the HeLa cells were treated with ALA (500 μM) for 24 h to enhance the GSH concentration. To decrease GSH concentration in living cells, HeLa cells were treated with NEM (500 μM) for 20 min. Both cell lines were washed for three times with cell culture media and incubated with MnO_2-CQDs nanocomposites (20 μg mL^{-1}) for 3 h. The cell lines were further washed with cell culture media and subsequently imaged at ambient temperature.

To further investigate the capacity of the probe to distinguish the normal cells and cancer cells, HepG2, HeLa and L02 cells were incubated with MnO_2-CQDs nanocomposites (20 μg mL^{-1}) for 3 h. The cell lines were then washed with cell culture media and imaged at ambient temperature.

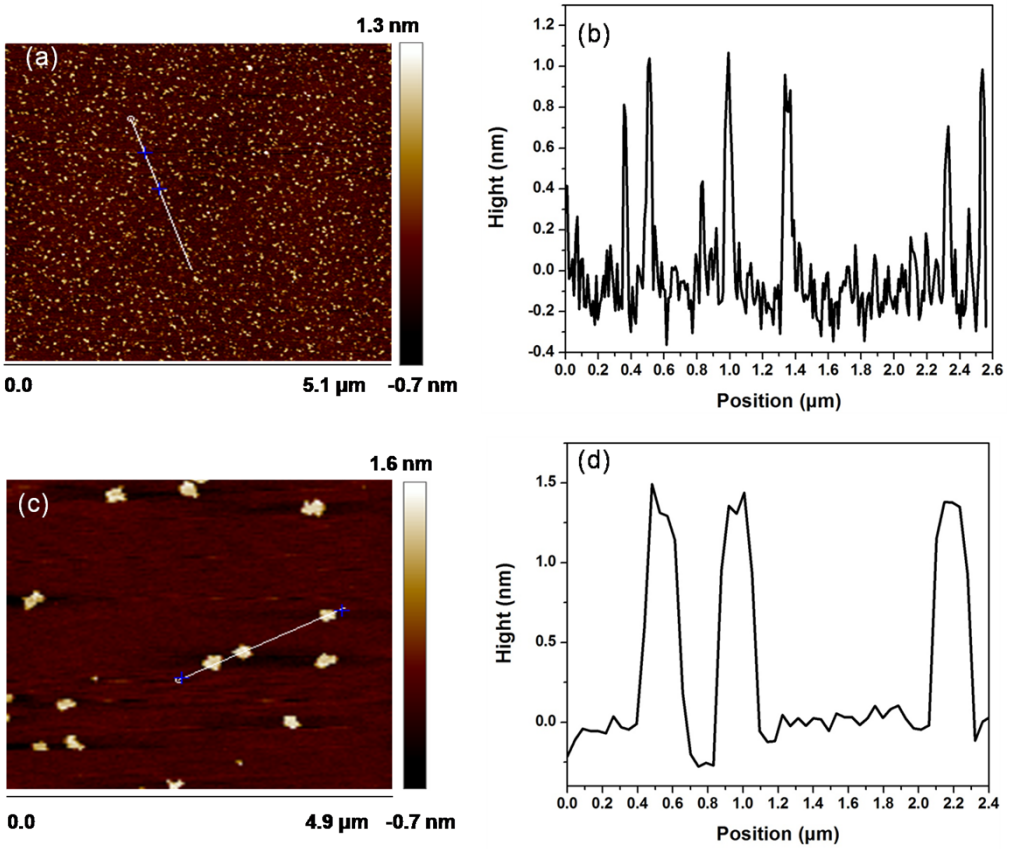

Fig. S1 AFM images of CQDs (a, b) and single-layer MnO_2 nanosheets (c, d) deposited on mica substrates.

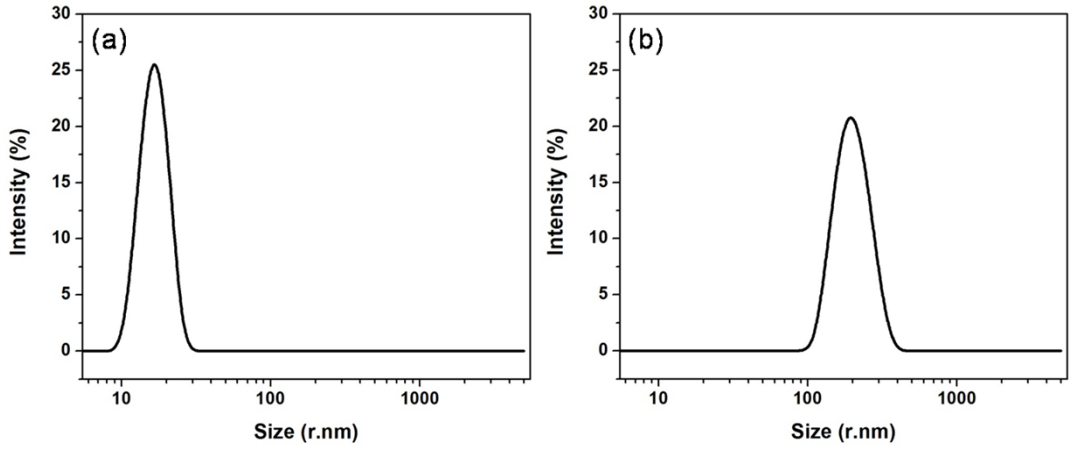

Fig. S2 DLS results of fluorescent CQDs (a) and single-layer MnO_2 nanosheets (b).

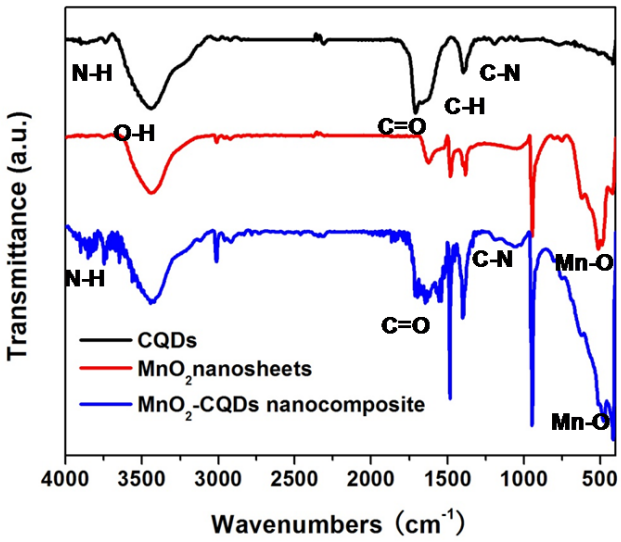

Fig. S3 FT-IR of CQDs, MnO_2 nanosheets and MnO_2-CQDs nanocomposite.

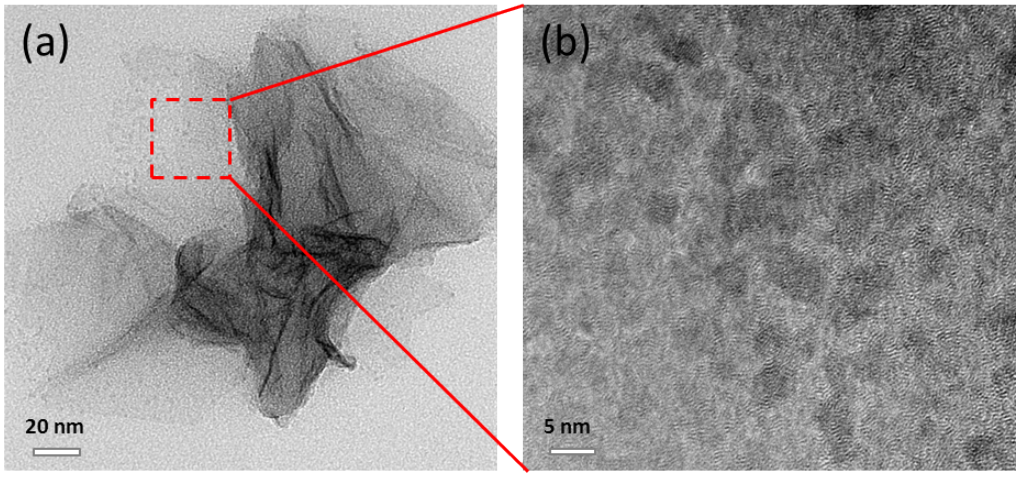

Fig. S4 TEM (a) and high-resolution TEM (b) images of MnO_2-CQDs nanocomposite.

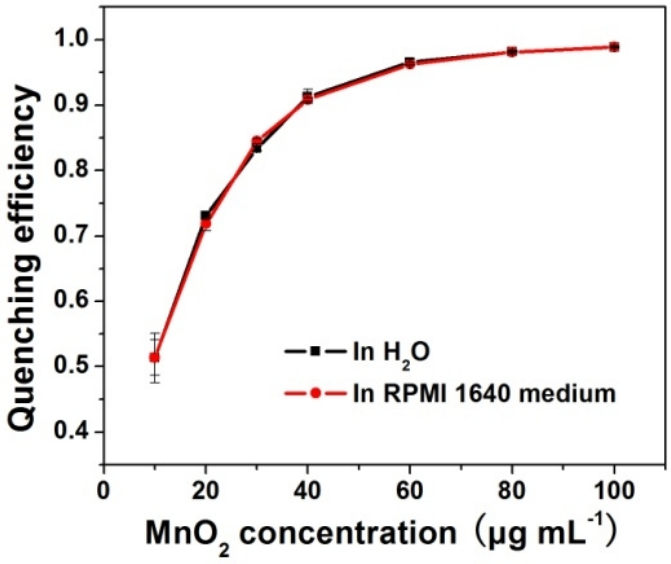

Fig. S5 The fluorescence quenching efficiency of the different concentrations of MnO_2 nanosheets toward CQDs in H_2O (black) and RPMI 1640 medium (red). $(F_0-F)/F_0$ as a function of MnO_2 concentrations. F and F_0 are fluorescence intensities of CQDs solutions with and without MnO_2 nanosheets, respectively.

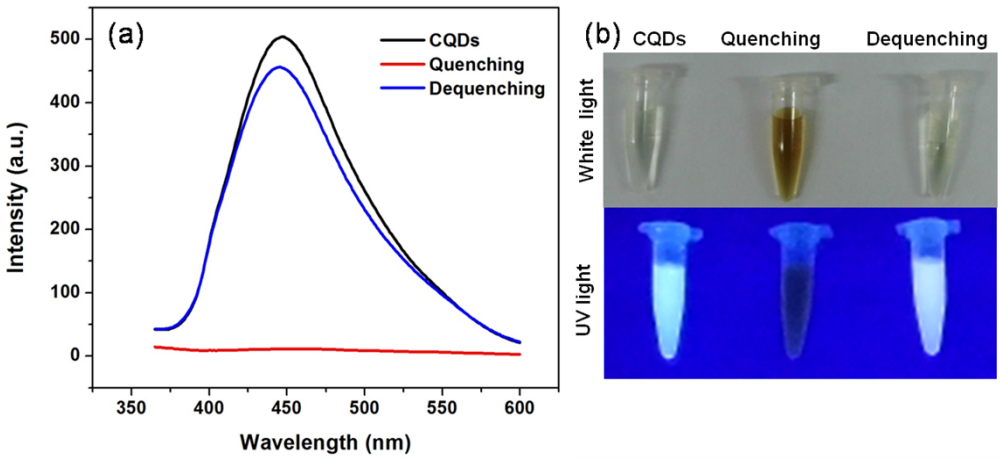

Fig. S6 Fluorescence emission spectra (a) and the white light/UV irradiation digital photographs (b) of fluorescent CQDs, quenching CQDs and dequenching CQDs solution.

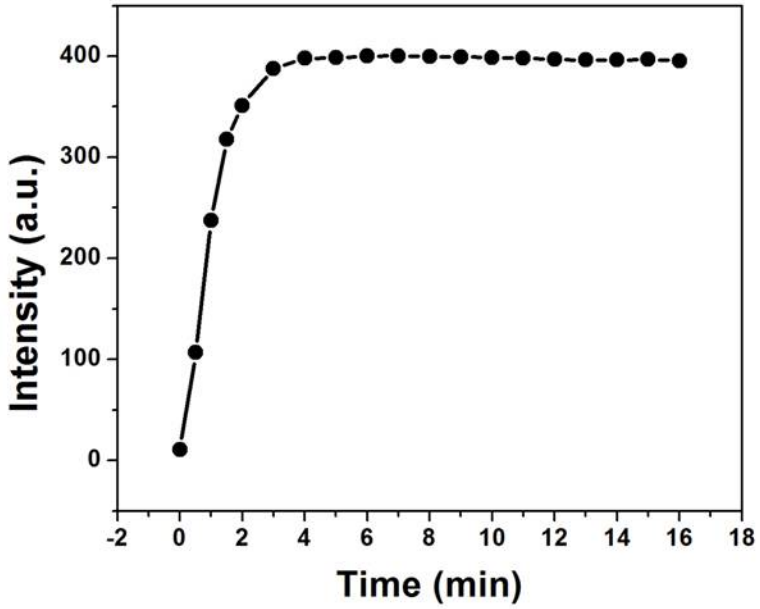

Fig. S7 Time dependence of fluorescence intensity at 447 nm for the MnO_2-CQDs nanocomposites in the presence of GSH (1 mM).

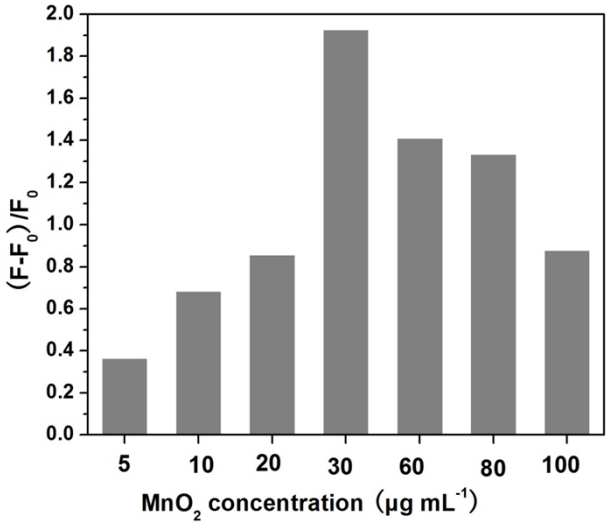

Fig. S8 Optimization of MnO_2 concentration for GSH sensing. F_0 is the fluorescence emission intensity of CQDs (2.4 μg mL^{-1}) in the presence of MnO_2 nanosheets; F is that in the presence of MnO_2 nanosheets and GSH (100 μM).

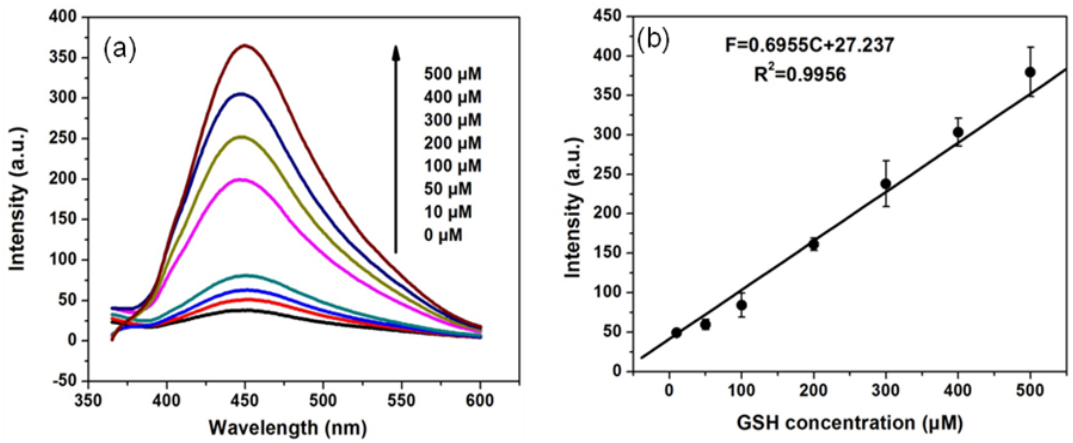

Fig. S9 (a) Fluorescence emission spectra of probe with use of 60 μg mL^{-1} MnO_2 nanosheets in the presence of different GSH concentrations. (b) The plot of the fluorescence intensities versus GSH concentrations.

The approach using 60 μg mL^{-1} MnO_2 nanosheets showed a lower fluorescence background than that using 30 μg mL^{-1} MnO_2 nanosheets. By the addition of GSH, the fluorescence of CQDs quenched by MnO_2 nanosheets was restored. The fitted curve could be used for the quantification of GSH with a correlation coefficient of 0.9956. And the detection limit as low as 1.71 μM could be reached based on the definition of three times the deviation of the blank signal (3σ).

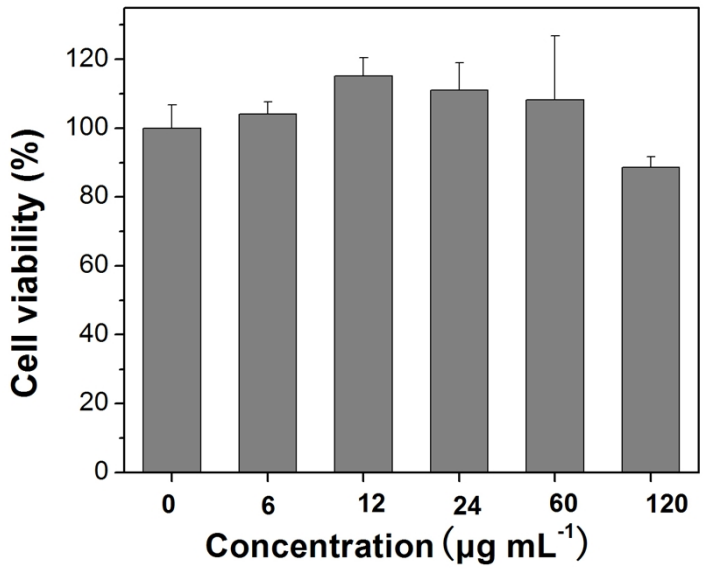

Fig. S10 Viability of HeLa cells after being incubated with different concentrations of CQDs for 24 h.

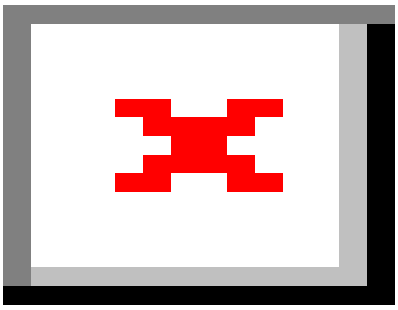

Fig. S11 CLSM images of HepG2, HeLa and L02 cells after being incubated with MnO_2-CQDs nanocomposite (20 μg mL^{-1}) for 3 h. Top row of images show fluorescence microscopy images; bottom row of images show the overlap of fluorescence and bright-field images. The scale bar is 20 μm.

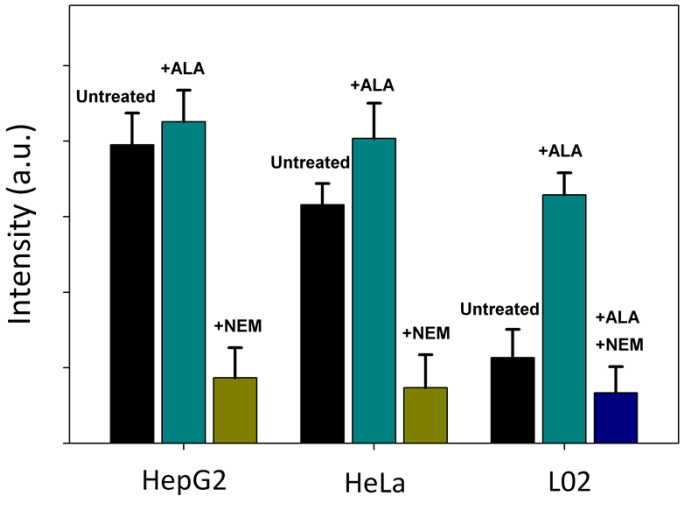

Fig. S12 Photoluminescence intensities of HepG2, HeLa and L02 cells measured after treatment with different chemicals and MnO_2-CQDs nanocomposites**.**

Table S1. Comparison of Different Fluorescence Methods for GSH Sensing.

probe	principle	linear range	LOD	note	ref.
Coumarin-malonitrile conjugate	Michael addition	no give	no give	complicated operation, special equipment, poor photostability	3
organoselenium fluorescent probe	selenium-nitrogen bond	0.015-1.0 μM	144 pM	complicated operation, time-consuming, require purification	4
naphthalimide-based colorimetric fluorescent probe	disulfide bonds	0.5-10 mM	28 μM	low sensitivity, complicated operation, time-consuming	5
CdSe-ZnSQDs-MV^{2+}	metal complexes-displace coordination	5-250 μM	0.6 μM	complicated operation, time-consuming, inherent toxicity	6
CdTe-Hg(II)	metal complexes-displace coordination	0.6-20 μM	0.1 μM	inherent toxicity, chemical instability	7
g-CNQDs-Hg^{2+}	metal complexes-displace coordination	0.16-16 μM	37 nM	rigorous pH conditions, toxic heavy metal, disable for cellular assay	8
Fe_3O_4@PFR@Au nanocomposites	metal complexes-oxidation-reduction	0.8-10 μM	0.5 μM	costly material, low sensitivity, rigorous pH conditions	9
MnO_2-modified UCNPs	GSH-decomposable MnO_2 nanosheets	no given	0.9 μM	low sensitivity, special equipment, complicated operation	10
g-C_3N_4-MnO_2	GSH-decomposable MnO_2 nanosheets	200-500 μM	0.2 μM	sophisticated technique, complicated operation, high temperature	11
MnO_2-CQDs nanocomposites	GSH-decomposable MnO_2 nanosheets	1-200 μM	10 nM	high sensitivity, good biocompatibility, no label, low cost	**this work**

References

1 K. Kai, Y. Yoshida, H. Kageyama, G. Saito, T. Ishigaki, Y. Furukawa and J. Kawamata, *J. Am. Chem. Soc.,* 2008, **130**, 15938-15943.

2 S. Qu, X. Wang, Q. Lu, X. Liu and L. Wang, *Angew. Chem. Int. Ed.*, 2012, **51**, 12215-12218.

3 H. Kwon, K. Lee and H.-J. Kim, *Chem. Commun*., 2011, **47**, 1773-1775.

4 B. Tang, L. Yin, X. Wang, Z. Chen, L. Tong and K. Xu, *Chem. Commun.*, 2009, 5293-5295.

5 B. Zhu, X. Zhang, Y. Li, P. Wang, H. Zhang and X. Zhuang, *Chem. Commun.*, 2010, **46**, 5710-5712.

6 J. Liu, C. Bao, X. Zhong, C. Zhao and L. Zhu, *Chem. Commun.*, 2010, **46**, 2971-2973.

7 B. Han, J. Yuan and E. Wang, *Anal. Chem.*, 2009, **81**, 5569-5573.

8 Y. Xu, X. Niu, H. Zhang, L. Xu, S. Zhao, H. Chen and X. Chen, *J. Agric. Food Chem.* 2015, **63**, 1747-1755.

9 P. Yang, Q. Xu, S. Jin, Y. Zhao, Y. Lu, X. Xu and S. Yu, *Chem. Eur. J.*, 2012, **18**, 1154-1160.

10 R. Deng, X. Xie, M. Vendrell, Y.-T. Chang, X. Liu, *J. Am. Chem. Soc.*, 2011, **133**, 20168-20171.

11 X. Zhang, C. Zheng, S. Guo, Juan Li, H. Yang and G. Chen, *Anal. Chem.*, 2014, **86**, 3426-3434.